Bond-orientational anisotropy in metallic glasses observed by x-ray diffraction

Y. Suzuki,* J. Haimovich,† and T. Egami
Department of Materials Science and Engineering and Laboratory for Research on the Structure of Matter, University of Pennsylvania, Philadelphia, Pennsylvania 19104
(Received 24 September 1986)

The structural anisotropy in metallic glasses induced by mechanical creep was observed by x-ray diffraction, using energy-dispersive x-ray diffractometry. The creep-induced anisotropy is the origin of the anelasticity in metallic glasses. The structural anisotropy was analyzed in terms of the anisotropic structure factor and anisotropic pair distribution function. The results show that the observed anisotropy is due to the atomic-bond-orientational anisotropy.

I. INTRODUCTION

Even though metallic glasses should be isotropic in the ideal state, various experimental observations suggest the presence of structural anisotropy in real glasses. In particular, the anelastic behavior, including anelastic recovery, reported on many metallic glasses,[1-5] indicates that the structural anisotropy can be induced by mechanical deformation. During creep deformation a part of the deformation energy can be stored as the structural anisotropy, or the anelastic polarization, and is released upon annealing under zero stress, causing anelastic recovery. The creep-induced structural anisotropy manifests itself also in the creep-induced magnetic anisotropy.[6-8] However, there has been no direct structural observation of the anisotropy due to anelastic polarization. The purpose of this paper to report on the first observation of such anisotropy by x-ray diffraction,[9] and to explain the result in terms of the atomic-bond-orientational anisotropy.

Structural anisotropy in metallic glasses has been reported by Windsor *et al.*[10] and by Suzuki,[11] both by neutron scattering. However, in both cases the anisotropy reported apparently was introduced during the preparation of the sample, rather than introduced later in a controlled manner, such as by mechanical deformation. Furthermore, the structural anisotropy was determined by comparing the diffraction intensities in the transmission and reflection geometries. This method, however, tends to be subject to various spurious effects such as the multiple-scattering. A more controlled study of structural anisotropy has been reported on colloid suspensions under shear, as they develop steady-state structural anisotropy, or undergo various phase transitions, from liquid to crystal, or from one crystalline structure to the other. In this work[12,13] the distortion in the structure was studied by light scattering, and analyzed in terms of the anisotropic structure factor.

II. EXPERIMENTAL METHODS

Since the structural anisotropy is expected to be very small, the energy-dispersive x-ray diffraction (EDXD) method[14,15] has been used in detecting such an anisotropy. In the EDXD method white x rays are used as the incident beam, and the spectrum of the diffracted x rays is measured by a solid-state detector at a constant diffraction angle. The structure factor is determined from the spectral modulation by the sample due to diffraction. Since the energy resolution of a solid-state detector is only marginally high (about 10^{-2} at 30 keV), the method is not suited to accurate lattice-constant measurements. However, it is a convenient method for fast structural study[16] or for the structural study of glasses[14,15] for which high resolution of the diffraction vector $\mathbf{Q}$ is not required. The main merits of the method are high photon counting rates which improve the statistics and allow the determination of small changes in the diffraction spectra, and the wide range of Q which improves the spatial resolution of the atomic pair distribution function (PDF) which is derived by the Fourier transformation of the structure factor. The method has been successfully used to study the effects of structural relaxation in metallic glasses.[14]

As a source of x rays, a rotating-anode x-ray generator with a Mo anode (Rigaku RU-200), operated at 50 kV and 100 mA, was used. The diffracted beam was detected by an intrinsic Ge detector (EG&G Ortex GLP) and the spectrum was compiled in a multichannel analyzer (Tracor-Northern 1700). The sample used was a ribbon of VITROVAC-4040, made by Vacuumschmeltze, with a composition of $Fe_{40}NI_{40}Mo_3Si_{12}B_5$ and a dimension of 35 μm$\times$15 mm$\times$70 mm.

The sample was annealed at 300 °C for 24 h in a vacuum of 10^{-5} Torr, under a tensile stress of 800 MPa, which is about $\frac{1}{4}$ to $\frac{1}{3}$ of the tensile strength. Another piece of ribbon was annealed in the same condition but without a stress, and was used as a control specimen. The total elongation of the sample after the stress annealing was about 3%.

The total structure factor and PDF of the as-received sample were determined from the diffraction spectrum obtained in reflection geometry, at diffraction angles $2\theta=7°$, 10°, 15°, 20°, 30°, 40°, and 60°, using the standard EDXD analysis procedure.[14,15] The structure factor $S(Q)$ and the reduced radial distribution function $G(r)=4\pi r[\rho(r)-\rho_0]$, where $\rho(r)$ is the pair density correlation function, or the pair distribution function, and ρ_0 is the average number density of the solid, are shown in Figs. 1 and 2. The structural anisotropy was determined by com-

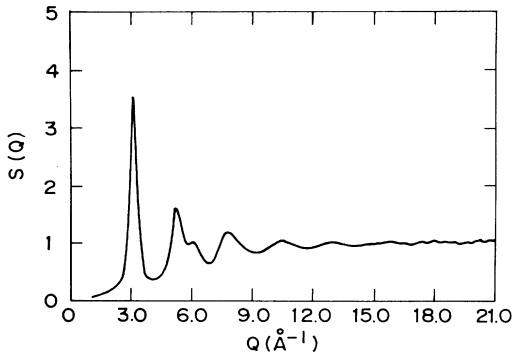

FIG. 1. Structure factor $S(Q)$ of amorphous $Fe_{40}Ni_{40}Mo_3Si_{12}B_5$ determined by energy-dispersive x-ray diffraction.

paring the diffraction spectra with the diffraction vector parallel, $I_{||}(E)$, or perpendicular, $I_{\perp}(E)$, to the direction of the tensile stress, where E is the photon energy, measured in transmission geometry at two diffraction angles, $2\theta=15°$ and 25°. In order to minimize the effect of drift in the electronic equipment, several short runs (typically 5×10^3 sec each) were repeated with alternating sample directions, and the counts were later summed up. The total exposure time was about 1×10^4 sec each, and the measurements were made for two sets of as-received and stress-annealed samples. While transmission geometry is necessary to keep both ($||$ and $\perp$) diffraction vectors in the plane of the sample, which allows more accurate determination of the anisotropy, it is more difficult to derive the structure factor from diffraction spectra obtained in transmission geometry, because of the stronger energy dependence of various factors such as the absorption factor. We have therefore determined the energy-dependent correction factors by directly comparing the data obtained in transmission geometry with the data obtained in reflection geometry which can be more accurately related to the structure factor.

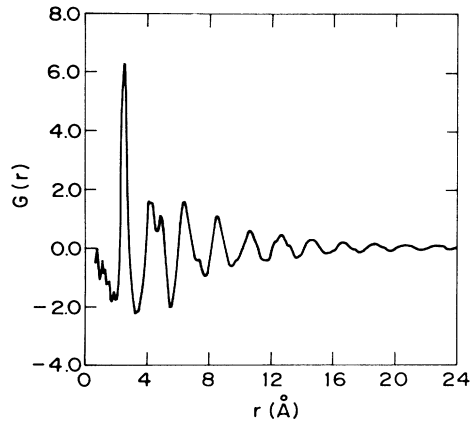

FIG. 2. Reduced radial distribution function $G(r)$ of amorphous $Fe_{40}Ni_{40}Mo_3Si_{12}B_5$ obtained by the Fourier transformation of the structure factor given in Fig. 1.

III. ANISOTROPIC STRUCTURE FACTOR

The diffraction spectra at $2\theta=15°$ and 25° and the anisotropy in the diffraction spectra, $\Delta I(E)=I_{||}(E)-I_{\perp}(E)$, are shown in Figs. 3 and 4. Since Q is related to E by

$$Q=\frac{4\pi}{hc}E\sin\theta=1.014E\sin\theta\ , \tag{1}$$

where Q is in $Å^{-1}$ and E is in keV, these spectra cover the Q range of 0 to 6.35 $Å^{-1}$ ($2\theta=15°$) and 0 to 10.53 $Å^{-1}$ ($2\theta=25°$). The sharp peaks at around 8 keV are due to fluorescent radiation from Fe and Ni, and two peaks at 17.4 and 19.6 keV are the $K\alpha$ and $K\beta$ radiations from Mo in the sample. These fluorescence lines should cancel each other when the difference spectra are taken, but they do not cancel perfectly, due to instrumental drift and other errors such as surface effects. However, the errors indicated by the lack of full cancellation of the fluorescent lines are sufficiently small and do not affect the results in which we are interested. These spectra clearly show that the samples annealed under stress are anisotropic and exhibit some structure near the first and second peaks of the structure factor, while the as-received and control samples are nearly isotropic. In fact, some of the as-received samples were found to be anisotropic, but we used those

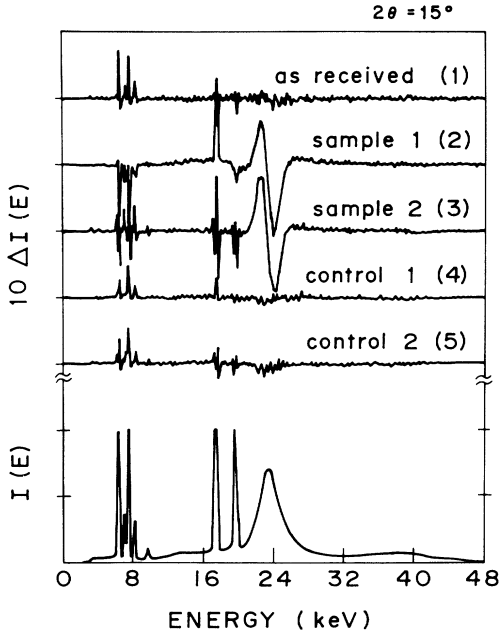

FIG. 3. The EDXD diffraction spectrum of amorphous $Fe_{40}Ni_{40}Mo_3Si_{12}B_5$ at $2\theta=15°$ (bottom), and the spectral anisotropy, $I_{||}(E)-I_{\perp}(E)$, for five samples: as-received (1), annealed at 300 °C under a stress of 800 MPa for 24 h (2) and (3), and annealed in the same condition but without a stress (4) and (5).

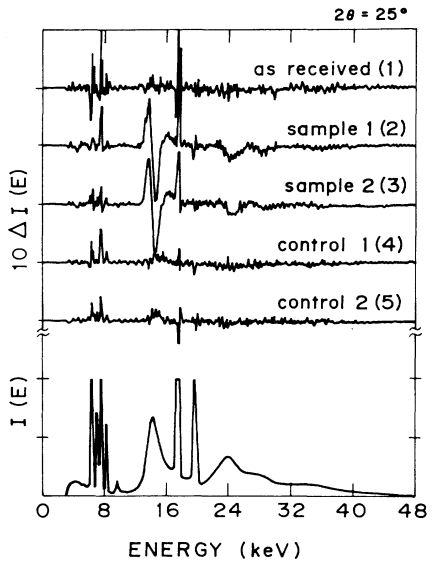

FIG. 4. Data similar to Fig. 3, but at $2\theta=25°$.

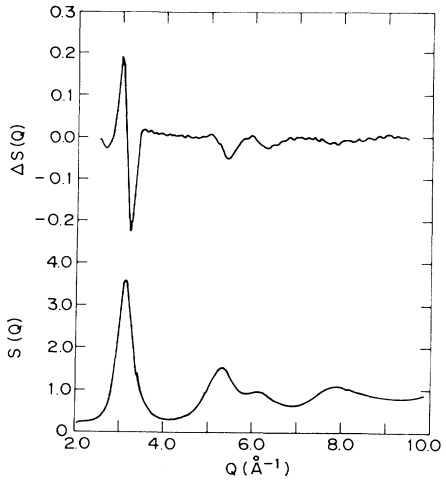

FIG. 5. Anisotropic structure factor $\Delta S(Q)$ compared with the structure factor $S(Q)$ of the as-received state (isotropic).

which are nearly isotropic for further study. Upon additional annealing treatments without stress, which promote the recovery of the anelastic polarization, $\Delta I(E)$ was observed to become smaller, following the $\ln t$ kinetics.[9] Such $\ln t$ kinetics are expected from the wide distribution of the relaxation times for recovery[3] and from the similar kinetics for the induction of the magnetic anisotropy due to anelastic polarization.[8] Therefore, this observation indicates that the observed structural anisotropy is indeed due to anelastic polarization.

In order to describe the anisotropy or the directional dependence of the structure factor and the pair distribution function, they may be expanded in spherical harmonics as

$$S(\mathbf{Q})=\sum_{l,m} S_l^m(Q)Y_l^m(\hat{\mathbf{Q}}) , \tag{2}$$

$$\rho(\mathbf{r})=\sum_{l,m} \rho_l^m(r)Y_l^m(\hat{\mathbf{r}}) , \tag{3}$$

where $\hat{\mathbf{Q}}=\mathbf{Q}/Q$ and $\hat{\mathbf{r}}=\mathbf{r}/r$. It can be readily shown that the coefficients in (2) and (3) are related to each other by

$$S_l^m(Q)=4\pi(i)^l \int \rho_l^m(r)\mathcal{J}_l(Qr)r^2dr , \tag{4}$$

$$\rho_l^m(r)=\frac{(i)^l}{2\pi^2} \int S_l^m(Q)\mathcal{J}_l(Qr)Q^2dQ , \tag{5}$$

where $\mathcal{J}_l(x)$ is the spherical Bessel function. Thus if we neglect the anisotropy terms higher than $l=2$, the anisotropic PDF can be obtained by

$$\Delta\rho(r)=-\frac{1}{2\pi^2} \int \Delta S(Q)\mathcal{J}_2(Qr)Q^2dQ , \tag{6}$$

where

$$\Delta\rho(r)=\rho(r_{\parallel})-\rho(r_{\perp})=\left[\frac{45}{16\pi}\right]^{1/2}\rho_2^0(r) , \tag{7}$$

$$\Delta S(Q)=S(Q_{\parallel})-S(Q_{\perp})=\left[\frac{45}{16\pi}\right]^{1/2}S_2^0(Q) . \tag{8}$$

The anisotropic structure factor $\Delta S(Q)$ is compared with $S(Q)$ in Fig. 5. In the region of the first peak of $S(Q)$, $\Delta S(Q)$ resembles the derivative of $S(Q)$ with respect to Q. In the region of the second and third peaks, however, the peak positions for $S(Q)$ and $\Delta S(Q)$ approximately agree. A more detailed comparison of $\Delta S(Q)$ and $dS(Q)/dQ$, which was determined from $S(Q)$ by numeri-

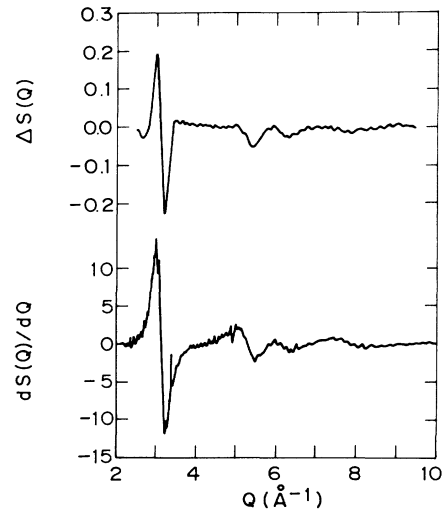

FIG. 6. $\Delta S(Q)$ compared with $dS(Q)/dQ$, obtained by the numerical differentiation of $S(Q)$.

cal differentiation, is shown in Fig. 6. It is observed that $\Delta S(Q)$ is indeed similar to $dS(Q)/dQ$ in the region of the first peak at around 3 Å^{-1}, but over a narrow range. Only the central position of the derivative of the first peak is proportional to $\Delta S(Q)$. As has been discussed by Cargill,[17] the central portion of the first peak of the structure factor describes the medium-range atomic correlation in real space, beyond the first peak of the PDF, while the second peak and the portions beyond the second peak of $S(Q)$ define the short-range order, particularly the nearest-neighbor peak of the PDF. As discussed in the following section, this implies that the medium-range atomic correlation is characterized by a uniform shear strain. The nearest-neighbor correlation, on the other hand, indicates the bond-orientational anisotropy.

IV. ANISOTROPIC PAIR DISTRIBUTION FUNCTION

A. Anisotropy due to uniform strain

The anisotropic PDF in terms of $\Delta G(r)=4\pi r\Delta\rho(r)$ and $G(r)$, together with $\Delta G(r)$ expected for the solid under uniform shear strain, $dG(r)/d\varepsilon$, are shown in Fig. 7. The peaks in $\Delta G(r)$ do not match at all with those in $G(r)$, but instead, $\Delta G(r)$ in the region beyond 4 Å strongly resembles $dG(r)/d\varepsilon$. The anisotropic PDF for uniform strain was calculated in the following manner. If we assume an axial shear strain along the z axis given by

$$\underline{\varepsilon}=\frac{1}{3}\begin{bmatrix}-\varepsilon & 0 & 0\\ 0 & -\varepsilon & 0\\ 0 & 0 & 2\varepsilon\end{bmatrix}, \tag{9}$$

the change in the PDF is

$$\frac{d\rho(\mathbf{r})}{d\varepsilon}=-\mathrm{div}[\rho(\mathbf{r})\mathbf{v}(\mathbf{r})]$$

$$=-\mathrm{grad}[\rho(\mathbf{r})\cdot\mathbf{v}(\mathbf{r})]-\rho(\mathbf{r})\mathrm{div}[\mathbf{v}(\mathbf{r})]\,, \tag{10}$$

where $\mathbf{v}=d\mathbf{r}/d\varepsilon$. For pure shear $\mathrm{div}[\mathbf{v}(\mathbf{r})]=0$. If the initial state is isotropic, for the strain given by (9) we obtain

$$\frac{d\rho(\mathbf{r})}{d\varepsilon}=-\left[\frac{16\pi}{45}\right]^{1/2}r\frac{d\rho(r)}{dr}Y_2^0(\hat{\mathbf{r}})\,. \tag{11}$$

Therefore, the anisotropic PDF of a solid under the shear strain is given by

$$\rho_2^0(r)=-\left[\frac{16\pi}{45}\right]^{1/2}r\frac{d\rho_0(r)}{dr}\varepsilon\,, \tag{12}$$

where $\rho_0(r)$ is the isotropic ($l=0$) PDF, and

$$\frac{dG(r)}{d\varepsilon}=r^2\frac{d}{dr}\left[\frac{G(r)}{r}\right], \tag{13}$$

which is shown in Fig. 7. From Eq. (4) we obtain

$$S_2^0(Q)=\left[\frac{16\pi}{45}\right]^{1/2}Q\frac{dS_0(Q)}{dQ}\varepsilon\,. \tag{14}$$

Thus the anisotropic structure factor of the solid under a shear strain is proportional to the derivative of the isotropic structure factor, as mentioned earlier.

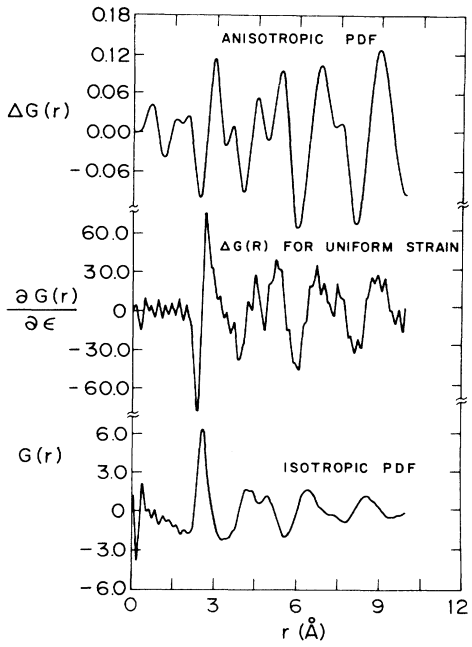

FIG. 7. The anisotropic PDF $\Delta G(r)$ (top), $dG(r)/d\varepsilon$ (middle), and the isotropic PDF $G(r)$ (bottom). See text for the method of obtaining $dG(r)/d\varepsilon$.

In order to confirm these results, we also carried out a computer simulation. The model structure we used is that of amorphous iron, originally produced by Maeda and Takeuchi, and used in various structural analysis and simulation studies.[18–21] The model consists of 2067 atoms interacting via a modified Johnson potential[22] and contained in a cubic cell with periodic boundary conditions. The model was deformed by modifying the boundary conditions corresponding to 3% shear strain, and internally relaxing the atomic structure. The anisotropic part of the PDF and that of the structure factor obtained by the Fourier transformation of the PDF are shown in Fig. 8. The same quantities obtained using Eqs. (13) and (14) are virtually identical to these, and both of them are very similar to those given in Figs. 6 and 7.

These results indicate that the anisotropy in the medium- to long-range (beyond 4 Å) atomic correlation is characterized by the uniform shear strain. This conclusion is reasonable since the deformation induced by creep is macroscopically uniform. Furthermore, the magnitude of the uniform strain, estimated by comparing $\Delta S(Q)$ with $dS(Q)/d\varepsilon$ using Eq. (14), is 0.5∼0.8%, which is comparable to the magnitude of recoverable strain which is about 1% for the present creep conditions. However, it should be emphasized that a solid anelastically polarized by creep deformation is not *elastically* deformed, since the structural study was performed in the stress-free state. How can the "uniform shear strain" be sustained without a stress? To resolve this apparent para-

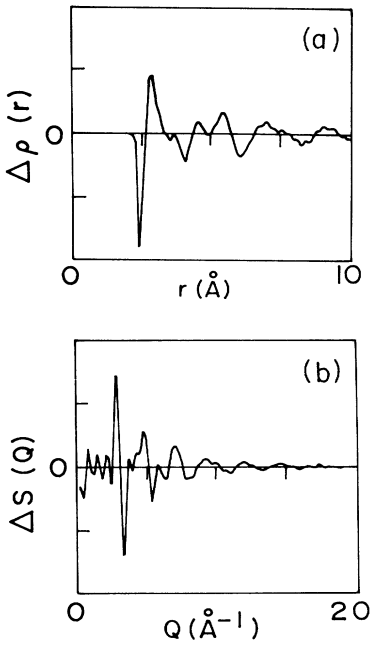

FIG. 8. The anisotropic PDF due to uniform elastic deformation (above) and the calculated anisotropic structure factor (below), both obtained by computer simulation.

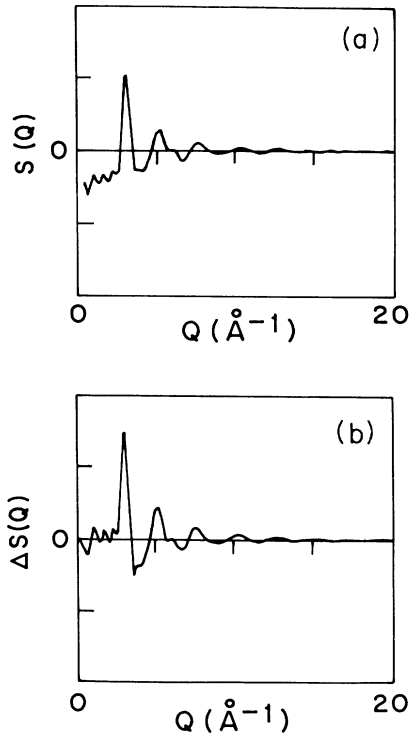

FIG. 9. The isotropic structure factor $S_0(Q)$ (above) and the anisotropic structure factor $\Delta S(Q)$, calculated by Eq. (18) for bond-orientational anisotropy, for the computer model.

dox, we should consider the possibility of bond-orientational anisotropy.

B. Bond-orientational anisotropy

Another type of structural anisotropy which can result in the anisotropic PDF is the bond-orientational anisotropy. In metallic glasses the definition of the atomic bond is somewhat arbitrary. However, since the first-nearest-neighbor peak of the PDF is relatively well separated from the second peak, the atomic bond can be defined as existing only between nearest-neighbor atoms. The orientational distribution of such bonds can be spatially anisotropic under certain circumstances. For instance, if a larger number of bonds is found to be aligned in the direction of the z axis than in the x and y axes, the anisotropic PDF may be given by

$$\rho_2^0(r)=\varepsilon_b\rho_0(r)\ , \tag{15}$$

at least for the first peak. Then the anisotropic structure factor is

$$S_2^0(Q)=-4\pi\varepsilon_b\int\rho_0(r)\mathcal{J}_2(Qr)r^2dr\ , \tag{16}$$

which is approximately proportional to $S_0(Q)$, as shown by the computer simulation in Fig. 9. Here the anisotropic structure factor has been calculated by Eq. (16) using the PDF of the model, and is compared to $S_0(Q)$ for the same model. Thus the agreement in the peak positions between $\Delta S(Q)$ and $S(Q)$ for the second and third peaks as shown in Fig. 5 is best explained in terms of the bond-orientational anisotropy. The magnitude of the bond-orientational anisotropy strain ε_b is about 5%. It should be noted that the sign of ε_b is *negative*, as can be determined by comparing Figs. 5 and 9. This means that more bonds are found in the direction *perpendicular* to the stress, somewhat contrary to what we might expect naively.

V. MICROSCOPIC MECHANISMS

The state of the deformation determined from the foregoing analysis is schematically summarized in Fig. 10. In the nearest-neighbor (NN) shell, more bonds are oriented perpendicular to the direction of the stress. Farther neighbors, however, are uniformly deformed along the axis of the stress, as if they were elastically deformed. This state of the bond-orientational anisotropy is not difficult to explain. It means that during the deformation some bonds were cut in the direction of the tensile stress, while new additional bonds were formed in the perpendicular direction. An example of such an atomic rearrangement is shown in Fig. 11. The orientations of the four peripheral bonds are also slightly changed by the rearrangement, but the effect of the bond exchange far outweighs them. Another way of explaining this effect is shown in Fig. 12. The isotropic NN distribution (a) becomes anisotropic under stress due to elastic deformation

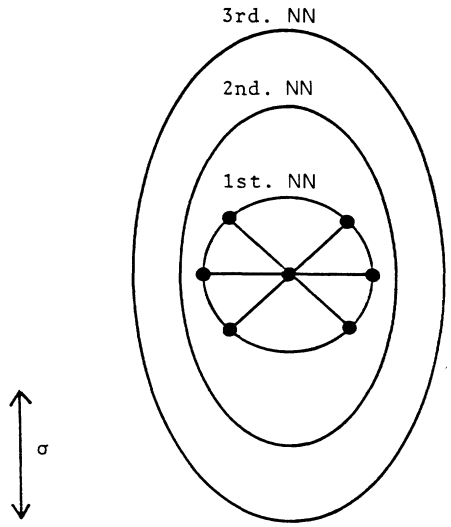

FIG. 10. Schematic representation of the microscopic state of anelastic polarization. The bond-orientational anisotropy is seen for the nearest neighbors in such a way that fewer bonds are oriented in the direction of the tensile stress, while for the second neighbors and beyond, the deformation is uniform as in the case of elastic deformation.

(b). But the interatomic potential is still isotropic, so that the system tries to recover isotropy under stress by severing bonds in the axial direction and forming new bonds in the planar direction (c). Thermal excitations may be necessary to achieve such rearrangements. When the stress is removed, however, *what was isotropic under stress becomes anisotropic without the stress* (d).

In covalently bonded systems such as polymers, the bond-orientational anisotropy will be induced by reorienting the existing bonds, so that as a result of mechanical deformation, *more* bonds will be found in the direction of the stress. In metallic glasses, on the other hand, bonds are much more easily cut and formed. Because of the negative curvature of the interatomic potential in the region between the first and second neighbors, if an atom is pulled away sufficiently from another atom, it suddenly

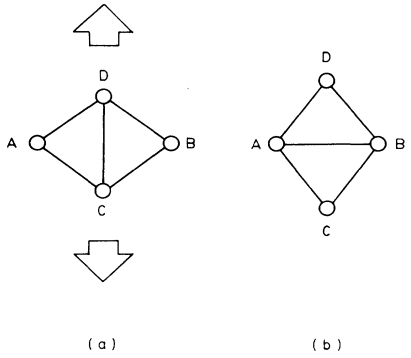

FIG. 11. Deformation of double triangles resulting in the bond exchange and the bond-orientational anisotropy.

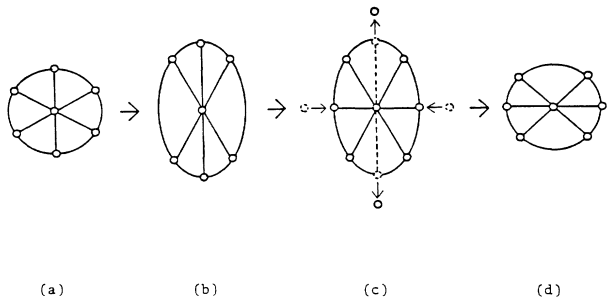

FIG. 12. Mechanism of producing bond-orientational anisotropy as a result of anelastic creep deformation. The isotropic bond distribution (a) becomes anisotropic under elastic stress (b). Then bond reformations or rearrangements would occur to make the bond distribution more isotropic under stress (c). When the stress is removed, the bond distribution is anisotropic (d).

changes from the first neighbor to the second neighbor. Such rearrangements are frequently seen during the simulation of deformation by a computer.[21,23] Therefore, in metallic glasses the bond-orientational anisotropy is produced not by the reorientation of the existing bonds, but by cutting old bonds and forming new bonds. Consequently *fewer* bonds are found in the direction of the tensile stress after deformation.

The effect of the bond-orientational anisotropy is short range, and in the medium range beyond the first NN the deformation should be uniform elongation along the z axis, as observed in the anisotropic PDF. The same phenomena can be viewed another way: As we mentioned earlier, such uniform deformation would result in an elastic stress which acts to reduce the z dimension. But this stress can be cancelled by the back stress due to the bond-orientational anisotropy, which counteracts to increase the z dimension so that the bond distribution becomes isotropic again. The anelastically polarized state can be preserved because of the balance between these two types of stresses. These arguments fully explain the observed anisotropic PDF in terms of the bond-orientational anisotropy, and suggest that the microscopic mechanism of anelasticity in metallic glasses is the local reformation of the atomic bonds which would result in the bond-orientational anisotropy.

VI. CONCLUSIONS

A detailed diffraction study was carried out on the structural anisotropy induced by mechanical creep deformation on a metallic glass $Fe_{40}Ni_{40}Mo_3Si_{12}B_5$. The anisotropic structure factor was determined by the energy-dispersive x-ray diffraction technique, by comparing the diffraction spectra with the diffraction vector parallel and perpendicular to the direction of the tensile stress. The anisotropic pair distribution function was derived from the anisotropic structure factor by a spherical Bessel transformation. The results can be satisfactorily interpreted in terms of the bond-orientational anisotropy, in such a way that more bonds are oriented in directions per-

pendicular to the axis of the tensile stress. It is concluded that the microscopic mechanism of anelasticity in metallic glasses is the local bond reformation which produces bond-orientational anisotropy.

ACKNOWLEDGMENTS

The authors are grateful to Dr. C. D. Graham, Jr. and Dr. V. Vitek for useful comments and suggestions. The work was supported by the U.S. Office of Naval Research through Grant No. N00014-80-C-0896. The research was conducted in part using the facilities of the Laboratory for Research on the Structure of Matter, University of Pennsylvania, supported by the National Science Foundation through Materials Research Laboratory Grant No. DMR-82-16718.

---

*Present address: Central Research Laboratory, Hitachi Corp., Tokyo, Japan.

†Present address: AMP Inc., Harrisburg, PA.

[1]R. Maddin and T. Masumoto, Mater. Sci. Eng. **9**, 153 (1972).

[2]B. S. Berry, in *Metallic Glasses,* edited by J. J. Gilman and H. J. Leamy (American Society for Metals, Metals Park, Ohio, 1978), p. 161.

[3]A. S. Argon and H. Y. Kuo, J. Non-Cryst. Solids **37**, 241 (1980).

[4]A. S. Argon, Phys. Chem. Solids **43**, 945 (1982).

[5]N. Morito and T. Egami, Acta Metall. **32**, 603 (1984).

[6]O. V. Nielsen and H. J. V. Nielsen, J. Magn. Magn. Mater. **22**, 21 (1980).

[7]H. R. Hilzinger, in *Proceedings of the 4th International Conference on Rapidly Quenched Metals,* edited by T. Masumoto and K. Suzuki (Japan Institute of Metals, Sendai, 1982), Vol. 2, p. 791.

[8]T. Jagielinski and T. Egami, IEEE Trans. Mag. **MAG-21**, 2005 (1985).

[9]Preliminary reports have been published in J. Haimovich, T. Jagielinski, and T. Egami, J. Appl. Phys. **57**, 3581 (1985); Y. Suzuki, J. Haimovich, and T. Egami, J. Phys. (Paris) Colloq. **46**, C8-623 (1985).

[10]C. G. Windsor, D. S. Boudreaux, and M. C. Narasimhan, Phys. Lett. **67A**, 282 (1978).

[11]K. Suzuki, in *Proceedings of the 4th International Conference on Rapidly Quenched Metals,* edited by T. Masumoto and K. Suzuki (Japan Institute of Metals, Sendai, 1982), Vol. 1, p. 309.

[12]N. A. Clark and B. J. Ackerson, Phys. Rev. Lett. **44**, 1005 (1980).

[13]B. J. Ackerson and N. A. Clark, Physica **118**, 221 (1983).

[14]T. Egami, J. Mater. Sci. **13**, 2589 (1978).

[15]T. Egami, in *Glassy Metals I,* edited by H.-J. Güntherodt and H. Beck (Springer, Berlin, 1981), p. 25.

[16]M. Mantler and W. Parrish, in *Advances in X-ray Analysis,* edited by H. F. McMurdie, C. S. Barrett, J. B. Newkirk, and C. O. Ruud (Plenum, New York, 1976), Vol. 20, p. 171.

[17]G. S. Gargill III, Solid State Phys. **30**, 227 (1975).

[18]K. Maeda and S. Takeuchi, J. Phys. F **8**, L283 (1978).

[19]D. Srolovitz, K. Maeda, S. Takeuchi, T. Egami, and V. Vitek, J. Phys. F **11**, 2209 (1981).

[20]D. Srolovitz, T. Egami, and V. Vitek, Phys. Rev. B **24**, 6936 (1981).

[21]Y. Suzuki and T. Egami, J. Non-Cryst. Solids **75**, 361 (1985).

[22]T. Egami and V. Vitek, in *Amorphous Materials: Modeling of Structure and Properties,* edited by V. Vitek (The Metallurgical Society of AIME, Warrendale, Pennsylvania, 1983), p. 127.

[23]Y. Suzuki, Ph.D. thesis, University of Pennsylvania, 1985 (unpublished).